has been seen in related optical studies of MgO:$LiNbO_3$ ferroelectric crystals (*15*). The electric field images presented earlier, though revealing and self-consistent, cannot address this question. However, the field effect—a direct measure of ferroelectric switching—gives a clear answer. The observed change in resistance of the $SrRuO_3$, lying 4000 Å below the level where the AFM had been used to write, indicates uniform switching of the ferroelectric polarization in the vertical direction. Finally, we have also used this structure to show that this writing procedure can be performed down to dimensions of 3500 Å. A 3500 Å wide line, whose width was determined from phase imaging, was traced along the length of the structure, resulting in a 0.5% change in the resistance. The calculated percent change is also 0.5%. Writing wider lines (8500 Å and 1.35 μm) revealed larger resistance changes that also scaled with area.

In principle, our method should enable the writing of electronic features as small as the radius of curvature of the AFM tip, a few hundred angstroms; recently, features as small as 1700 Å have been written (*16*). This approach is generally applicable to many classes of materials, given the strong progress that has been made in the thin-film deposition of epitaxial oxide films. It can be applied directly to many perovskite oxide systems, including the high-temperature superconductors, to investigate superconducting field effect devices as well as Josephson field effect devices and arrays (*17*). Also, because the heteroepitaxial growth of ferroelectric PZT, $BaTiO_3$, and related oxides has been demonstrated on single-crystal Si and GaAs, it should be possible to extend this approach to semiconductor structures, where the carrier densities are orders of magnitude smaller than in $SrRuO_3$ (*3, 18*).

REFERENCES AND NOTES

1. J. F. Scott and C. A. Paz de Araujo, *Science* **246**, 1400 (1989).
2. R. Ramesh *et al., ibid.* **252**, 944 (1991); C. B. Eom *et al., ibid.* **258**, 1766 (1992); C. H. Ahn *et al., ibid.* **269**, 373 (1995); Y. Watanabe, *Appl. Phys. Lett.* **66**, 1770 (1995).
3. C. B. Eom *et al., Appl. Phys. Lett.* **63**, 2570 (1993).
4. C. H. Ahn *et al., ibid.* **70**, 206 (1997).
5. F. Saurenbach and B. D. Terris, *ibid.* **56**, 1703 (1990); R. Lüthi *et al., J. Appl. Phys.* **74**, 7461 (1993).
6. T. Hidaka *et al., Appl. Phys. Lett.* **68**, 2358 (1996).
7. J. E. Stern, B. D. Terris, H. J. Mamin, D. Rugar, *ibid.* **53**, 2717 (1988).
8. J. Massanell, N. Garcia, A. Zlatkin, *Opt. Lett.* **21**, 12 (1996); O. Kolosov *et al., Phys. Rev. Lett.* **74**, 4309 (1995).
9. C. H. Ahn *et al.,* in preparation. The deposition rate was ~5 Å s^{-1} and the substrate temperature was held at 660°C, with atomic oxygen provided to the sample at a background pressure of 2×10^{-5} torr.
10. J.-M. Triscone *et al., J. Appl. Phys.* **79**, 4298 (1996). The deposition rate was ~0.1 Å s^{-1}, and the substrate temperature was held at 530°C, with a background pressure of 0.2 torr of oxygen and argon (P_{O_2}/P_{Ar} = 40%).
11. The nominal radius of curvature for the metallized tips used in this experiment is ~500 Å, and the spring constant is 1 to 5 N m^{-1}. The tip amplitude used was ~300 Å.
12. In this grounded mode of operation, the response of the cantilever is invariant to the polarity of the ferroelectric, always being attractive. Squares written with positive voltages appear as depressions, as do squares written with negative voltages.
13. The sign of the observed contrast in these images for a given reading bias shows that the electrostatic interaction between the tip and surface results from an overscreening of the surface after the ferroelectric polarization has switched, similar to what is observed in electret materials with aligned dipolar moments [G. M. Sessler, Ed., *Electrets* (Springer-Verlag, Berlin, 1980)]. From the bias voltage needed to reverse the contrast of these images (<1 V magnitude), we estimate that this excess screening charge density represents a small fraction (<1%) of the induced ferroelectric polarization charge density.
14. We believe that area B gave the most reproducible changes in resistance because there were a few dust particles present on the otherwise featureless surface, making it easier to locate the same area for poling. Areas A and C were more difficult to locate reproducibly, and the variations in step height for the staircase in Fig. 5A may be largely attributable to difficulties in locating exactly the same areas, potentially leading to overlap between the poled regions.
15. A. Kuroda, S. Kurimura, Y. Uesu, *Appl. Phys. Lett.* **69**, 1565 (1996).
16. T. Tybell *et al.,* in preparation.
17. J. Mannhart, *Supercond. Sci. Technol.* **9**, 49 (1996).
18. K. Nashimoto, D. K. Fork, T. H. Geballe, *Appl. Phys. Lett.* **60**, 1199 (1992).

19. We thank M. Decroux, S. R. Manalis, L. Miéville, S. C. Minne, C. F. Quate, J. W. Reiner, and S. Reymond for useful discussions and technical advice. Supported by the Swiss National Science Foundation and the U.S. Air Force Office of Scientific Research.

21 January 1997; accepted 17 March 1997

Disordered Biopyriboles, Amphibole, and Talc in the Allende Meteorite: Products of Nebular or Parent Body Aqueous Alteration?

Adrian J. Brearley

Transmission electron microscope observations of the Allende carbonaceous chondrite provided evidence of widespread hydrous phases replacing enstatite in chondrules. Calcic amphibole and talc occur in thin (less than 0.3 micrometer) crosscutting veins and as alteration products of primary chondrule glass in contraction cracks within the enstatite. In addition, talc and disordered biopyriboles were found replacing enstatite grains along cracks and fractures. Although rare hydrous phases have been reported in calcium- and aluminum-rich inclusions in the Allende meteorite, these observations suggest that aqueous fluids played a much more significant role in the mineralogical and geochemical evolution of Allende than has previously been thought.

Carbonaceous chondrites are among the most primitive of solar system materials and provide important clues into processes such as evaporation, condensation, and melting, which took place in the earliest stages of the formation of our solar system (*1*). Many carbonaceous chondrites have experienced aqueous alteration at low temperatures (*2*), but the location and timing of these reactions are controversial. For example, the rare hydrous phases found in some calcium- and aluminum-rich inclusions (CAIs) and chondrules (*3–7*) in the Allende CV3 carbonaceous chondrite have been attributed to both preaccretionary (nebular) and postaccretionary (parent body) (*7*) hydrous alteration reactions. A resolution of the timing and location of aqueous alteration would improve our understanding of nebular processes and the evolution of the parent bodies of carbonaceous chondrites.

This study reports high-resolution transmission electron microscope (HRTEM) observations of pyroxene-rich chondrules in Allende, which show that the effects of aqueous alteration are more widespread than previously recognized. Seven porphyritic pyroxene chondrules from a single thin section of Allende were selected for study by TEM (*8*). In all seven chondrules, the dominant phase is clinoenstatite ($En_{93-98}Wo_1$), with subordinate olivine (Fa_{1-10}) sometimes constituting up to 30 modal percent of the chondrule (Fig. 1). The clinoenstatite in all three chondrules has been extensively replaced by FeO-rich olivine (Fa_{29-45}) (*9–12*), and primary MgO-rich olivines invariably have narrow rims (<15 μm) of FeO-rich olivine surrounding them. Glass in all chondrules has been replaced by a fine-grained (<50 μm) assemblage of minerals that were not studied in detail but include nepheline and sodalite (*13*).

Analysis by HRTEM showed that the development of hydrous phases is widespread in all seven chondrules but is consistently restricted to the phenocrysts of

Institute of Meteoritics, Department of Earth and Planetary Sciences, University of New Mexico, Albuquerque, NM 87131, USA.

clinoenstatite. Although the degree of alteration is minor, the hydrous phases present and the alteration textures are identical in all the chondrules. Veins, typically ~0.2 μm wide, filled with fibrous minerals were observed crosscutting the clinoenstatite crystals (Fig. 2A). Analysis of the vein-filling phases by selected-area electron diffraction, HRTEM, and x-ray microanalysis showed that they are talc with calcic amphibole [composition close to that of magnesiohornblende with Mg/(Mg + Fe) = ~0.80] (Table 1) and minor anthophyllite, which have replaced the clinoenstatite topotaxially, such that the (100) planes of both phases are coincident. Randomly oriented talc and amphibole have also developed in contraction fractures within the clinoenstatite that were probably originally filled with glass (*14*) (Fig. 2B). The veins of hydrous phases do not appear to crosscut FeO-rich olivine, but amphibole and talc occur as inclusions within the olivine itself.

HRTEM imaging of clinoenstatite grains parallel to the *c* axis has shown that regions of highly disordered biopyriboles are sometimes present associated with grains of talc (Fig. 3A). These regions consist of clinoenstatite interlayered with randomly stacked chains ranging from three to eight chains in width (Fig. 3B). So far, only a single lamella of a recognizable ordered biopyribole has been observed, consisting of a layer of jimthompsonite, three unit cells in thickness. The disordered biopyriboles have complex structures, changing from double or triple to multiple chains when followed along the *a* axis.

In terrestrial rocks, biopyriboles form during the retrograde hydration of enstatite to amphibole and talc and are regarded as metastable intermediate reaction products in the transformation (*15*). There are remarkable microstructural similarities between the replacement textures in Allende and those in terrestrial biopyriboles. These results indicate that the transformation has occurred by the same mechanism, providing evidence that hydrous fluids have interacted to a limited extent with all the chondrules studied. Although hydrous phases, such as phlogopite, chlorite margarite, clintonite, potassium-rich mica, and montmorillonite, have been reported in CAIs and chondrules in Allende (*3–6*), they are extremely rare. This overall lack of evidence for hydration in Allende has been interpreted as evidence for preaccretionary alteration of some components in the nebula (*1–3*). In contrast, on the basis of studies of dark inclusions in Allende (*16*), it has been suggested that Allende itself has been aqueously altered and then metamorphosed within a parent body (*7, 16*). Thus, the observation of widespread, although limited, hydrous phases in chondrules has important implications for these two models. In the parent body model, FeO-rich olivine (*9–12*) is the product of the dehydration of phases such as Fe-rich serpentine (*5*). The low bulk H_2O content (<0.1 weight %) of Allende (*17*) and the rarity of hydrous phases could plausibly be attributed to complete or partial dehydration during metamorphism.

The assemblage and textural relations of the hydrous phases provide important constraints on the conditions, timing, and location of alteration, relative to the formation of FeO-rich olivine in Allende. Although veins of talc and amphibole crosscut chondrule clinoenstatite, they are not present within FeO-rich olivine that has replaced the enstatite itself. In addition, inclusions of amphibole also occur within the FeO-rich

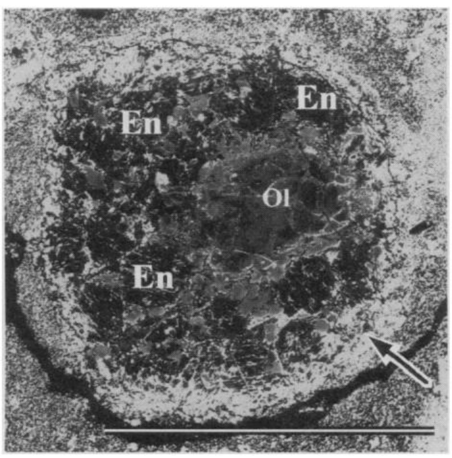

Fig. 1. Backscattered electron image of a pyroxene-rich chondrule examined in this study. The chondrule consists of phenocrysts of clinoenstatite (dark phase, labeled En), associated with a large, zoned forsteritic olivine crystal (Ol). Smaller olivine grains are distributed within the chondrule. The periphery of the chondrule shows the presence of a characteristic rim (arrow) and the localized replacement of clinoenstatite by FeO-rich olivine. Bar, 1 mm.

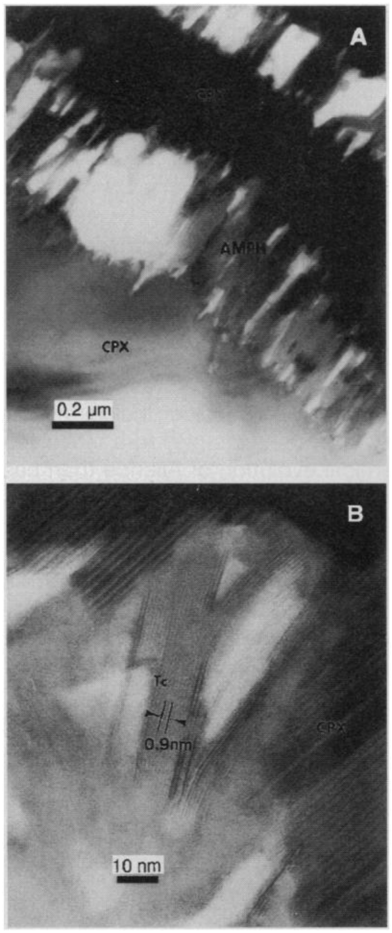

Fig. 2. (**A**) Low-magnification TEM image showing veins of fibrous Ca-rich amphibole (AMPH), which have crosscut and have replaced clinoenstatite (CPX) in a chondrule. The amphibole is typically oriented with its (100) plane parallel to subparallel to the (100) plane of the altered enstatite. The white regions within the veins are holes produced during the ion-milling procedure used for sample preparation. (**B**) TEM image showing randomly oriented crystals of talc (Tc) that have grown within a contraction crack within enstatite (CPX) in a chondrule. The 0.9-nm (001) basal spacing of the talc is shown.

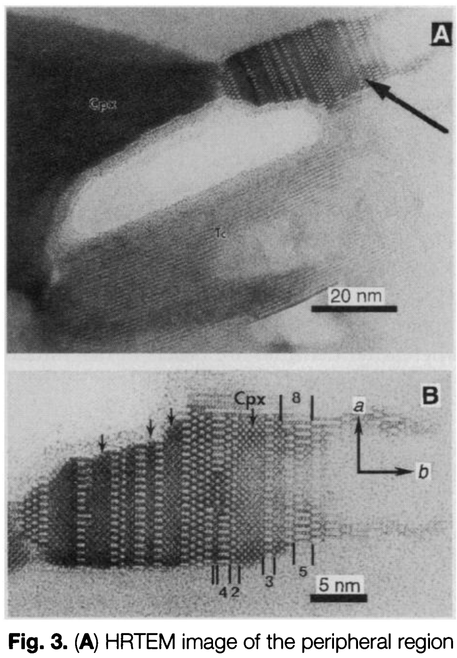

Fig. 3. (**A**) HRTEM image of the peripheral region of enstatite (Cpx) within a chondrule that has been partially replaced by talc (Tc) and biopyriboles (upper right, arrow), imaged with the electron beam parallel to the *c* axis. (**B**) Magnified HRTEM image of the region of biopyriboles shown in (A). The image is rotated relative to (A). The region consists of an intergrowth of enstatite with multiple–chain width biopyriboles. Lamellae with chain widths of between two (amphibole) and eight are present. In many cases the chain width repeat changes along the *a* direction of the chain, resulting in complex stacking arrangements of individual basic units.

olivine. These observations show that formation of the veins and the amphibole inclusions occurred either before or concurrently with the formation of the olivine. In addition, the alteration assemblage is different from that reported in any carbonaceous chondrite. In CI, CM, CO, and other CV chondrites the alteration mineralogy is dominated by phases such as saponite and Fe-rich serpentine [$(Mg,Fe)_3Si_2O_5(OH)_4$], consistent with low-temperature aqueous alteration, certainly below ~150°C (*2*, *18*). In contrast, the presence of talc and amphibole in the Allende chondrules is much more consistent with a higher temperature of alteration.

For a nebular model, the formation of FeO-rich olivine after, or closely associated with the occurrence of, the hydrous alteration of clinoenstatite would require a two-stage history in which chondrules first interacted with a water-bearing nebular gas at temperatures of around 200° to 300°C and pressures of 10^{-3} to 10^{-6} atm in order to partially hydrate enstatite (*19*). Nebular conditions must then become more oxidizing, accompanied by a significant increase in temperature (~1200 K) (*12*), such that FeO-rich olivine could form by condensation or metasomatism (*10–12*). Such high temperatures would have destroyed the hydrous phases present in Allende chondrules. Recent evidence suggests that a high-temperature origin for matrix FeO-rich olivine may, in any case, be problematical. These olivines contain submicrometer-sized inclusions of pentlandite (*20*), a phase that is not stable above 610°C. Thus, a nebular model appears to be inconsistent with the observations and would require a complex and unusual sequence of events. In addition, it would be a remarkable coincidence that seven randomly selected chondrules within one thin section all exhibit the same type and degree of alteration. For a nebular model, this would require alteration of all chondrules under identical conditions and times without their separation during accretion, a scenario that seems improbable.

The parent body model involving aqueous alteration and metamorphism needs to account for the survival of some hydrous phases relative to others. For example, if the primary hydrous alteration produced considerable quantities of serpentine, would this decompose during the proposed metamorphic event, while phases such as talc and amphibole survive? If the precursor of the FeO-rich olivine in Allende was some kind of serpentine (*8*), it was probably FeO-rich, having a composition similar to that of serpentines in CM chondrites (*21*). It is not possible to analyze the phase relations in this system rigorously, because the phase assemblage is not at thermodynamic equilibrium. Nevertheless, the relative stabilities of serpentine, talc, and amphibole can be determined from experimental and thermodynamic data. Experimental data show that at low pressures (1 bar) chrysotile dehydrates to form talc by the reaction chrysotile

$$[Mg_3Si_2O_5(OH)_4] \rightarrow \text{olivine}(Mg_2SiO_4)$$
$$+ \text{ talc } [Mg_6Si_8O_{20}(OH)_4] + H_2O$$

at ~250° to 300°C (*22*). The effect of Fe will be to lower the stability of serpentine further (*23*). Calculated phase equilibria show that talc and anthophyllite [$Mg_7Si_8O_{22}(OH)_2$] (*24*) are stable to significantly higher temperatures. The reaction anthophyllite → enstatite + quartz + H_2O occurs above 365°C, and talc breaks down to enstatite + quartz + H_2O at 379°C (*24*), constraining the maximum metamorphic temperatures to below ~340°C. This is consistent with the presence of pentlandite inclusions in matrix fayalitic olivine (*20*).

The conditions of the proposed initial episode of aqueous alteration in Allende are uncertain. On the basis of observations of other carbonaceous chondrites (*18*), talc, amphibole, and biopyriboles would not have formed if alteration occurred below ~150°C but represent a signature of a higher temperature alteration. One possible explanation is that these components are not related to the early phase of alteration but were actually produced during the metamorphic reactions that dehydrated the serpentine. The fluid released during the breakdown of serpentine at elevated temperatures, above 300°C, could have catalyzed the retrograde hydration of enstatite to produce biopyriboles, amphibole, and talc.

Table 1. Representative analytical TEM analyses of calcic amphibole.

Oxide	1	2	3
SiO_2	45.02	46.20	44.82
TiO_2		0.20	
Al_2O_3	11.90	12.41	12.53
Cr_2O_3	0.56	0.16	
FeO	7.37	6.78	6.54
MnO	0.42	0.22	
MgO	18.36	19.39	23.27
CaO	14.40	14.65	12.85
Total	100.00	100.00	100.00

Structural formulas based on the presence of 23 O atoms.

Element	1	2	3
Si	6.312	6.429	6.220
Ti		0.021	
Al	1.972	2.036	2.050
Cr	0.062	0.018	
Fe	0.865	0.789	0.759
Mn	0.050	0.026	
Mg	4.247	4.021	4.813
Ca	2.162	2.184	1.911
Mg/(Mg+Fe)	0.831	0.836	0.864

REFERENCES AND NOTES

1. G. J. MacPherson, D. A. Wark, J. T. Armstrong, in *Meteorites and the Early Solar System*, J. F. Kerridge and M. S. Matthews, Eds. (Univ. of Arizona Press, Tucson, 1988), pp. 746–807; J. N. Grossman, A. E. Rubin, H. Nagahara, E. A. King, *ibid.*, pp. 619–659.
2. D. J. Barber, *Clay Miner.* **20**, 415 (1985); L. P. Keller and P. R. Buseck, *Geochim. Cosmochim. Acta* **54**, 1155 (1990); K. Tomeoka and P. R. Buseck, *ibid.*, p. 1787.
3. K. Tomeoka and P. R. Buseck, *Nature* **299**, 326 (1982).
4. A. Hashimoto and L. Grossman, *Geochim. Cosmochim. Acta* **51**, 1685 (1987).
5. L. P. Keller and P. R. Buseck, *Science* **252**, 946 (1991).
6. M. Kimura and Y. Ikeda, *Meteoritics* **31**, A70 (1996).
7. A. N. Krot, E. R. D. Scott, M. E. Zolensky, *ibid.,* **30**, 738 (1995); A. N. Krot, E. R. D. Scott, M. E. Zolensky, *ibid.,* **32**, 31 (1997).
8. Doubly polished thin sections of Allende, mounted with an acetone soluble epoxy, Loctite 414, were prepared. Chondrules were selected by optical microscopy and characterized in detail by scanning electron microscopy and electron microprobe analysis. Slotted Cu grids were glued over chondrules of interest, and the samples were removed by immersion in acetone. These samples were prepared for TEM by ion-beam milling, with a Gatan ion beam mill. TEM was carried out on JEOL 2000FX and JEOL 2010 instruments, both operating at 200 kV. A Tracor Northern TN 5500 energy-dispersive x-ray analysis system was used to obtain in situ mineral analyses, with the Cliff-Lorimer thin-film approximation for data reduction. Experimental correction (*k* factors) was used throughout.
9. R. M. Housley and E. H. Cirlin, in *Chondrules and Their Origins*, E. A. King, Ed. (Lunar and Planetary Institute, Houston, TX, 1983), pp. 145–161.
10. J. A. Peck and J. A. Wood, *Geochim. Cosmochim. Acta* **51**, 1503 (1987).
11. X. Hua, J. Adam, H. Palme, A. El Goresy, *ibid.* **52**, 1389 (1988).
12. S. Weinbruch, H. Palme, W. F. Müller, A. El Goresy, *Meteoritics* **25**, 115 (1990).
13. K. Kimura and Y. Ikeda, *Proc. Nat. Inst. Polar Res. Symp. Antarct. Meteorites* **8**, 123 (1995).
14. M. Yasuda, M. Kitamura, N. Morimoto, *Phys. Chem. Miner.* **9**, 192 (1983).
15. D. R. Veblen and P. R. Buseck, *Am. Mineral.* **64**, 687 (1979); *ibid.* **65**, 599 (1980).
16. T. Kojima and K. Tomeoka, *Meteoritics* **28**, 649 (1993); *Geochim. Cosmochim. Acta* **60**, 2651 (1996).
17. R. S. Clarke, E. Jarosewich, J. Nelen, M. Gomez, J. R. Hyde, *Smithson. Contrib. Earth Sci.* **5**, 53 (1970).
18. M. E. Zolensky, T. Barrett, L. Browning, *Geochim. Cosmochim. Acta* **57**, 3123 (1993).
19. Y. Ikeda and M. Prinz, *ibid.*, p. 439.
20. A. J. Brearley and M. Prinz, *Lunar Planet. Sci.* **XVIII**, 161 (1996).
21. T. E. Bunch and S. Chang, *Geochim. Cosmochim. Acta* **44**, 1543 (1980).
22. J. V. Chernosky Jr., *Can. Mineral.* **20**, 19 (1982).
23. B. W. Evans and S. Guggenheim, *Reviews in Mineralogy: Hydrous Silicates* (Mineralogical Society of America, Washington, DC, 1988), vol. 17, pp. 225–294.
24. Stable breakdown reactions were calculated with the TWQ program [R. G. Berman, *Can. Mineral.* **29**, 833 (1991)] and the thermodynamic dataset [R. G. Berman, *J. Petrol.* **29**, 445 (1988)].

25. Electron microprobe analysis and TEM were carried out in the Electron Microbeam Analysis Facility, Department of Earth and Planetary Sciences and Institute of Meteoritics, University of New Mexico. Supported by NASA grant NAG 3347 (J. J. Papike).

17 October 1996; accepted 1 April 1997